Int. J. Heat Mass Transfer. Vol. 15, pp. 619–635. Pergamon Press 1972. Printed in Great Britain

RADIATING BOUNDARY LAYERS AT PLANETARY ENTRY VELOCITIES

MERWIN SIBULKIN and EZENWA A. DENNAR

Division of Engineering, Brown University, Providence, Rhode Island, U.S.A.

(*Received* 24 *February* 1971)

Abstract—Results are presented for constant pressure, laminar boundary layers for velocities at which thermal radiation may be important. When radiation effects are significant, the boundary layer profiles are nonsimilar and different solutions must be obtained for planar (flat plates, wedges) and axisymmetric (cones) flows. Using power law approximations to the gas properties and a new set of reference conditions, a hypersonic limit is defined which gives skin friction and heat transfer parameters that are independent of Mach number. For a particular gas and flow geometry (planar or axisymmetric), this approach gives a universal solution for the radiating boundary layer. It is found that although the convective and radiative heat fluxes vary strongly with distance from the leading edge, the total heat flux is nearly independent of position. For Earth reentry trajectories including returns from the far solar system it is shown that convection is the dominant mode of heat transfer in such boundary layers for vehicles of moderate size. Comparisons of the power law property solution with calculations using exact gas properties for air are presented and the range of agreement is discussed.

NOMENCLATURE

B_ν, Planck function;

$(c_f)_r$; $(c_f)_e$ $\tau_w/\frac{1}{2}\rho_r u_e^2$; $\tau_w/\frac{1}{2}\rho_e u_e^2$, skin friction coefficient;

c_p, specific heat at constant pressure;

E_n, exponential integrals;

F, $(2n+1)^{-\frac{1}{2}}(c_f)_r(Re_r)^{\frac{1}{2}}$, friction parameter;

h; $\tilde{h}$, static enthalpy; $= h/\frac{1}{2}u_e^2$;

k_{eq}, equilibrium thermal conductivity;

n, 0 for planar flow, $= 1$ for axisymmetric flow;

p, static pressure;

Pr_{eq}, equilibrium Prandtl number;

q^C, conductive heat flux;

q^R, radiative heat flux;

Q^C, $(2n+1)^{-\frac{1}{2}} st_r^C (Re_r)^{\frac{1}{2}}$ conductive heat transfer parameter;

Q_r^R, $(2n+1)^{-\frac{1}{2}} st_r^R (Re_r)^{\frac{1}{2}}$ radiative heat transfer parameter;

r, radius of body of revolution;

Re_r; Re_e, $\rho_r u_e x/\mu_r$; $\rho_e u_e x/\mu_e$, Reynolds number;

s, $(2n+1)^{-1}\rho_r\kappa_r\Gamma_r x$, nondimensional streamwise coordinate;

st_r^C; st_e^C, $q_w^C/\frac{1}{2}\rho_r u_e^3$; $q_w^C/\frac{1}{2}\rho_e u_e^3$, Stanton number for conduction;

st_r^R, $q_w^R/\frac{1}{2}\rho_r u_e^3$, Stanton number for radiation;

T, static temperature;

u; $\tilde{u}$, streamwise velocity component; $= u/u_e$;

v, normal velocity component;

x; y, streamwise coordinate; normal coordinate;

Γ_r, $\sigma T_r^4/\rho_r u_e h_r$, radiation–convection ratio;

ε, surface emissivity;

η; ξ, transformed coordinates defined by (5);

κ; κ_p, (mass) absorption coefficient; Planck mean;

μ, viscosity;

ρ, density;

τ, shear stress;

ϕ, $\rho\mu/\rho_r\mu_r$.

Subscripts

e,	boundary layer edge value;
r,	reference state;
w,	wall value;
ν,	spectral frequency.

1. INTRODUCTION

ONE OF the basic problems of laminar boundary layer theory is the analysis of the flow of a viscous fluid over a flat plate, or more precisely, over a constant pressure surface. As is well known, when the fluid density and viscosity are constant the momentum equation is independent of the energy equation and a similarity solution for the velocity profiles exists which was obtained by Blasius [1]. When the thermal conductivity is also constant, the corresponding similarity solution for the temperature profiles was obtained by Pohlhausen [2] for Prandtl numbers applicable to gases and to liquids such as water.

The next step in boundary layer theory was to extend the analysis to compressible flows in which the fluid transport properties varied. For high subsonic and low to moderate supersonic velocities the behavior of air is adequately described by a perfect gas equation of state with constant values of specific heat, and the natural nondimensional velocity parameter is the Mach number. The analysis of the constant pressure boundary layer equations (which for supersonic flow apply to wedges and cones as well as flat plates) still gives similarity solutions, but the accuracy of the results obtained, such as the skin friction and heat transfer coefficients, depends upon the values used for the transport properties.

In order to obtain the most accurate results it is usually necessary to sacrifice generality and mathematical simplicity. For example, at moderate Mach numbers, the most accurate solutions (Van Driest [3]) used the Sutherland viscosity formula, but a particular free-stream temperature had to be specified. Less accurate results were obtained by Karman and Tsien [4] using a power law approximation to the Sutherland viscosity formula, but these results are independent of the free-stream temperature. A significant gain in mathematical simplicity is obtained by the use of a linear viscosity-temperature relationship which for a perfect gas equation of state gives $\rho\mu = \text{constant}$ and leads to a transformed momentum equation (e.g. Stewartson [5]) which is identical to the constant property momentum equation. However, the solution of this equation gives a heat transfer coefficient which is independent of Mach number, a result which is far from accurate. For the case of an insulated wall this situation can be improved by the use of the Chapman and Rubesin [6] relation $\mu/\mu_\infty = C(T/T_\infty)$ where C is evaluated to give the correct viscosity at the wall, but it is not always realized that for the cold wall case, $T_w = T_\infty$, no improvement results.

At higher flight velocities ($u_\infty > 8000$ ft/s, say) air no longer behaves as a perfect gas, and because of the effects of dissociation and then of ionization the chemical composition of the fluid in the boundary layer is no longer constant. One must then consider the transfer of energy within the boundary layer due to diffusion of species. The general solution of this problem requires the addition of one or more species conservation equations to the set of boundary layer equations, but for the case of local chemical equilibrium the effects of variable composition can be handled by using a properly defined "equilibrium thermal conductivity" in the energy equation (e.g. Dorrance [7]). Using this approach and accurate empirical fits to the thermodynamic and transport properties of air, N. B. Cohen [8] computed solutions for the flat plate boundary layer for velocities up to 41 000 ft/s. His results, and those of many other investigations at lower velocities, show that the skin friction and heat transfer coefficients decrease continually as the velocity increases.

However, for sufficiently large velocities such that the inverse Mach number $M_\infty^{-1} \to 0$, it should be possible to formulate the problem in such a way that the results become indepent of free-stream velocity. (For wedge and cone boundary layers the significant parameter is

M_e^{-1}.) Results which are valid in this hypersonic limit have been obtained by Cohen and Reshotko [9] for a perfect gas using the relationship $\rho\mu$ = constant. Since, as discussed previously, the use of $\rho\mu$ = constant necessarily leads to a heat transfer coefficient which is independent of Mach number, Cohen and Reshotko's results do not provide a useful hypersonic limit for the boundary layer equations. In this paper we shall obtain such limiting hypersonic results for the equilibrium, laminar, constant pressure boundary layer by using, as a compromise between accuracy and generality, a set of power law approximations to the thermodynamic and transport properties of air.

The next significant complication of the boundary layer problem occurs at flight velocities for which radiation is important. It is sometimes erroneously believed that all flat plate boundary layers are similar because there is no finite characteristic physical length in the problem; when radiation is included, however, there is both a viscous "length" ν/u and a radiation "length" $(\rho\kappa)^{-1}$ and solutions of the constant pressure boundary layer equations are nonsimilar. In addition, as will be shown, it is no longer possible to transform two-dimensional (plates, wedges) and axisymmetric (cones) flows into identical equations. Since radiation is only important at extreme velocities, the concept of hypersonic limiting solutions will be used to eliminate the free-stream Mach number (or equivalent parameters such as the Eckert number) from the problem. As a consequence it will be found necessary to define Reynolds numbers and friction and heat transfer coefficients which are independent of the fluid properties at the edge of the boundary layer.

It has been known since the early work of Kàrmàn and Tsien [4] that at large Mach numbers the boundary layer velocity profile is roughly linear. For the cold wall case (which is the one of interest at extreme velocities), the velocity gradient changes rapidly near the wall and becomes singular in the limiting case of $T_w \to 0$. This has led to practical difficulties in calculating the skin friction and convective heat transfer coefficients (Sibulkin and Dispaux 1968) from a numerical solution of the boundary layer equations. To overcome this difficulty an extension of the momentum- and energy-integral equations will be derived in this paper from which these coefficients can be obtained without calculating the velocity and enthalpy gradients at the wall.

2. BOUNDARY LAYER EQUATIONS

The laminar boundary layer equations for steady flow over a constant pressure two-dimensional or axisymmetric surface are

$$\frac{\partial}{\partial x}(\rho u r^n) + \frac{\partial}{\partial y}(\rho v r^n) = 0, \tag{1}$$

$$\rho u \frac{\partial u}{\partial x} + \rho v \frac{\partial u}{\partial y} = \frac{\partial}{\partial y}\left(\mu \frac{\partial u}{\partial y}\right), \tag{2}$$

$$\rho u \frac{\partial h}{\partial x} + \rho v \frac{\partial h}{\partial y} = \frac{\partial}{\partial y}\left(\frac{k_{eq}}{c_p}\frac{\partial h}{\partial y}\right) + \mu\left(\frac{\partial u}{\partial y}\right)^2 - \nabla \cdot \boldsymbol{q}^R, \tag{3}$$

where the index $n = 0$ for two-dimensional flow and $n = 1$ for axisymmetric flow. For aerodynamic problems, where the pressure and internal energy of the radiation field can be neglected, the effect of radiation is given by the last term of the energy equation which represents the net energy per unit volume which is carried away by radiative transfer. The flow has been assumed to be in chemical equilibrium; for a reacting gas the equilibrium thermal conductivity k_{eq} is the sum of the heat conductivity due to conduction and to diffusion of atoms and molecules through the boundary layer (Dorrance [7], p. 74ff). Since the pressure has been assumed to be constant, the equations do not apply to regions where hypersonic viscous interaction effects are important or to regions which are influenced by nose bluntness.

The boundary layer equations may be put into a more convenient form by introducing a

stream function ψ which satisfies the continuity equation

$$\frac{\partial \psi}{\partial y} = \rho u r^n, \quad \frac{\partial \psi}{\partial x} = -\rho v r^n, \tag{4}$$

and using the coordinate transformation

$$\eta \equiv \frac{u_e r^n}{(2\zeta)^{\frac{1}{2}}} \int_0^y \rho \mathrm{d}y', \tag{5a}$$

$$\zeta \equiv \int_0^x \rho_r \mu_r u_e r^{2n} \mathrm{d}x'. \tag{5b}$$

This transformation is identical to the one used by Lees [10] and subsequent investigators except that a reference density ρ_r and a reference viscosity μ_r are used (for reasons which will be discussed below) instead of the density and viscosity at the edge of the boundary layer. After defining

$$f(\eta, \zeta) \equiv \frac{\psi}{(2\zeta)^{\frac{1}{2}}} \tag{6}$$

it follows that

$$\frac{u}{u_e} = \frac{\partial f}{\partial \eta} \tag{7}$$

for both similar and nonsimilar boundary layers. Then using (4)–(7) one can transform the boundary layers equations into the form

$$\frac{\partial}{\partial \eta}\left(\phi \frac{\partial^2 f}{\partial \eta^2}\right) + f \frac{\partial^2 f}{\partial \eta^2} = 2\zeta\left(\frac{\partial f}{\partial \eta}\frac{\partial^2 f}{\partial \zeta \partial \eta} - \frac{\partial f}{\partial \zeta}\frac{\partial^2 f}{\partial \eta^2}\right), \tag{8}$$

$$\frac{\partial}{\partial \eta}\left(\frac{\phi}{Pr_{eq}}\frac{\partial h}{\partial \eta}\right) + f\frac{\partial h}{\partial \eta} + u_e^2 \phi\left(\frac{\partial^2 f}{\partial \eta^2}\right)^2 = 2\zeta\left(\frac{\partial f}{\partial \eta}\frac{\partial h}{\partial \zeta} - \frac{\partial f}{\partial \zeta}\frac{\partial h}{\partial \eta}\right) + \frac{2\zeta \nabla \cdot \boldsymbol{q}^R}{\rho \rho_r \mu_r u_e^2 r^{2n}}, \tag{9}$$

where the nonsimilar terms have been collected on the right-hand side of the equations.

As discussed in the Introduction, when $h_e/\frac{1}{2}u_e^2 \ll 1$ it should be possible to obtain useful approximate results by going to the hypersonic limit $M_e^{-1} \to 0$. (For wedges and cones this approximation limits the results to small vertex angles.) In so doing we replace a real flow having boundary conditions u_e, p_e and h_e by an approximating flow having the same values of u_e and p_e but with $h_e = 0$. Consequently, the boundary conditions on density and viscosity in the approximating flow become $\rho_e = \infty$ and $\mu_e = 0$ making these quantities unsuitable for use as characteristic values in defining nondimensional quantities. We therefore define the characteristic values

$$h_r \equiv \tfrac{1}{2}u_e^2; \ \rho_r \equiv \rho(h_r, p_e), \quad \mu_r \equiv \mu(h_r, p_e), \ T_r \equiv T(h_r, p_e), \quad \kappa_r \equiv \kappa(h_r, p_e), \tag{10}$$

and the nondimensional variables

$$\equiv \tilde{u}/u_e; \ \tilde{h} \equiv h/h_r, \ \tilde{\rho} \equiv \rho/\rho_r, \ \ldots \ . \tag{11}$$

The radiation term in (9) can be simplified by noting that for our problem

$$\zeta / r^{2n} = (2n+1)^{-1} \rho_r \mu_r u_e x$$

and defining a nondimensional streamwise coordinate

$$s \equiv (2n+1)^{-1} \rho_r \kappa_r \Gamma_r x, \tag{12}$$

where $\Gamma_r \equiv \sigma T_r^4 / \frac{1}{2}\rho_r u_e^3$ is a characteristic radiation/convection ratio. Substituting (7) and (10)–(12) into (8) and (9) gives (using subscript notation for compactness)

$$[\phi \tilde{u}_\eta]_\eta + f\tilde{u}_\eta = \frac{2s}{2n+1}(\tilde{u}\tilde{u}_s - f_s \tilde{u}_\eta), \tag{13}$$

$$[(\phi/Pr_{eq})\tilde{h}_\eta]_\eta + f\tilde{h}_\eta + 2\phi\tilde{u}_\eta^2 = \frac{2s}{2n+1}(\tilde{u}\tilde{h}_s - f_s\tilde{h}_\eta) + \frac{2s}{\tilde{\rho}}\tilde{\nabla} \cdot \tilde{\boldsymbol{q}}^R, \tag{14}$$

$$f = \int_0^\eta \tilde{u} \mathrm{d}\eta' + f(0, s), \tag{15}$$

where $\tilde{\boldsymbol{q}}^R \equiv \boldsymbol{q}^R / \sigma T_r^4$ and $\tilde{\nabla} \equiv (\rho_r \kappa_r)^{-1} \nabla$. Because

the radiation term in (14) depends explicitly upon s, the solutions of these constant pressure boundary layer equations are nonsimilar and all the terms on the right-hand sides of (13) and (14) must be retained when radiation is significant.* Since these terms depend explicitly upon n, the solutions for planar flow ($n = 0$) and axisymmetric flow ($n = 1$) are no longer identical.

The momentum equation (8) has been reduced from a third order to a second order equation (13) by the use of $\tilde{u}$ as an independent variable and the auxiliary relation (15); this is in anticipation of subsequent numerical solution of these equations by the method of finite differences. Finally it should be noted that the usual explicit dependence of the energy equation on an external flow parameter such as Mach number or Eckert number has been eliminated in (14) by our choice of $\tilde{h} \equiv h/\frac{1}{2}u_e^2$ as the nondimensional enthalpy.

The boundary conditions on (13)–(15) for a constant temperature, permeable wall are

$$\begin{aligned} &\text{at } \eta = 0; \quad \tilde{u} = 0, \quad f = f(0, s), \quad \tilde{h} = \tilde{h}_w \\ &\text{at } \eta = \infty; \quad \tilde{u} = 1, \quad \tilde{h} = \tilde{h}_e. \end{aligned} \tag{16}$$

The approximation involved in going to the hypersonic limit $M_e^{-1} = 0$ consists of replacing the enthalpy conditions in (16) by

$$\tilde{h}_e = 0, \ \tilde{h}_w = 0. \tag{16a}$$

Since the equations themselves are independent of M_e, this is the only approximation which is made.

3. EVALUATION OF THE RADIATION TERM

For a flat plate all the radiative flux results from viscous heating in the boundary layer, while for a wedge or cone the gas between the boundary layer and the shock may provide an additional source of radiation. Since the entire shock layer is thin at flight conditions for which radiation is important, the radiation term div $\boldsymbol{q}^R$ is well approximated by the one-dimensional equations of radiative transfer. Then

$$\frac{1}{\tilde{\rho}} \tilde{\nabla} \cdot \tilde{\boldsymbol{q}}^R = \int_0^\infty \tilde{\kappa}_\nu \frac{\partial \tilde{q}_\nu}{\partial \tau_\nu} \mathrm{d}\nu, \tag{17a}$$

and (see, for example, Sparrow and Cess [12] Chap. 7),

$$\begin{aligned} \frac{\partial \tilde{q}_\nu}{\partial \tau_\nu} &= 4\pi \tilde{B}_\nu(\tau_\nu) \\ &\quad - 2\pi \int_0^\infty \tilde{B}_\nu(t_\nu) E_1(|\tau_\nu - t_\nu|) \mathrm{d}t_\nu - 2\tilde{q}_\nu^+(0) E_2(\tau_\nu) \end{aligned} \tag{17b}$$

where $\tilde{B}_\nu \equiv B_\nu/\sigma T_r^4$ and B_ν is the Planck function. For a black wall $\tilde{q}_\nu^+(0) = \pi B_\nu(T_w)$; for a diffusely emitting and reflecting wall $\tilde{q}_\nu^+(0) = \varepsilon_\nu \pi B_\nu(T_w) + (1 - \varepsilon_\nu)\tilde{q}_\nu^-(0)$ and the radiant flux striking the wall $\tilde{q}_\nu^-(0)$ is given by

$$\tilde{q}_\nu^-(0) = 2\pi \int_0^\infty \tilde{B}_\nu(\tau_\nu) E_2(\tau_\nu) \mathrm{d}\tau_\nu. \tag{18}$$

Using (5) and (12), the optical depth $\tau_\nu \equiv \int_0^y \rho \kappa_\nu \mathrm{d}y'$ is related to the boundary layer coordinates by

$$\tau_\nu = \frac{2^{\frac{1}{2}}(2n+1)^{\frac{1}{2}} s}{Re_r^{\frac{1}{2}} \Gamma_r} \int_0^\eta \tilde{\kappa}_\nu \mathrm{d}\eta'. \tag{19}$$

The radiative transfer aspect of the problem can be greatly simplified when the boundary layer and shock layer are optically thin and the wall is cold. Sibulkin and Dispaux [13] have shown that this is the case for continuum radiation in air at flight conditions up to 40 km/s; the effect of line radiation on these results is not known at this time. In this limit the radiation term in (14) reduces to (e.g. Sparrow and Cess [21]),

$$\frac{2s}{\tilde{\rho}} \tilde{\nabla} \cdot \tilde{\boldsymbol{q}}^R = 8 s \tilde{\kappa}_p \tilde{T}^4, \tag{20}$$

where $\tilde{\kappa}_P \equiv \kappa_P/\kappa_r$ and $\kappa_P \equiv (\pi/\sigma T^4) \int_0^\infty \kappa_\nu B_\nu \mathrm{d}\nu$ is the Planck mean (mass) absorption coefficient.

* It may be noted, in contrast with this result, that for the staganation point boundary layer (Howe and Viegas [11]) the radiation term is independent of ζ and consequently similar solutions exist for that problem.

4. AUXILIARY QUANTITIES

After solution of the boundary layer equations a number of auxiliary quantities may be obtained. In deriving these results repeated use is made of the relationship

$$\frac{\partial y}{\partial \eta} = \frac{2^{\frac{1}{2}}}{(2n+1)^{\frac{1}{2}}} \frac{x}{(Re_r)^{\frac{1}{2}}} \frac{1}{\tilde{\rho}}.$$

Thus the distance normal to the wall in the physical plane is given by

$$z \equiv (2n+1)^{\frac{1}{2}}(Re_r)^{\frac{1}{2}}(y/x)$$

$$= 2^{\frac{1}{2}} \int_0^{\eta} \tilde{\rho}^{-1} \mathrm{d}\eta'; \qquad (21)$$

the displacement thickness is given by

$$\Delta \equiv (2n+1)^{\frac{1}{2}}(Re_r)^{\frac{1}{2}}(\delta^*/x)$$

$$= 2^{\frac{1}{2}} \int_0^{\infty} [\tilde{\rho}^{-1} - (\rho_r/\rho_e)\tilde{u}] \mathrm{d}\eta, \qquad (22)$$

and the momentum thickness by

$$\Theta \equiv (2n+1)^{\frac{1}{2}}(Re_r)^{\frac{1}{2}}(\rho_e/\rho_r)(\theta/x)$$

$$= 2^{\frac{1}{2}} \int_0^{\infty} \tilde{u}(1-\tilde{u}) \mathrm{d}\eta, \qquad (23)$$

where the standard definitions of δ^* and θ have been used. In addition, an energy thickness

$$\Theta_H \equiv \int_0^{\infty} \frac{\rho u}{\rho_e u_e} \left(\frac{H_e - H}{u_e^2/2} \right) \mathrm{d}y$$

is defined where the stagnation enthalpy $H \equiv h + u^2/2$; the corresponding nondimensional form is

$$\Theta_H \equiv (2n+1)^{\frac{1}{2}}(Re_r)^{\frac{1}{2}}(\rho_e/\rho_r)(\theta_H/x)$$

$$= 2^{\frac{1}{2}} \int_0^{\infty} \tilde{u}(\tilde{H}_e - \tilde{H}) \mathrm{d}\eta. \qquad (24)$$

A modified skin friction coefficient $(c_f)_r \equiv \tau_w/\frac{1}{2}\rho_r u_e^2$ is defined to obtain a quantity which remains finite and non-zero in the hypersonic limit; its relationship to the velocity gradient at the wall is given by

$$F \equiv (2n+1)^{-\frac{1}{2}}(c_f)_r(Re_r)^{\frac{1}{2}} = 2^{\frac{1}{2}}[\phi \tilde{u}_\eta]_{\eta=0}. \qquad (25)$$

The corresponding convective Stanton number $st_r^C \equiv q_w^C/\frac{1}{2}\rho_r u_e^3$ is related to the enthalpy gradient at the wall by

$$Q^C \equiv (2n+1)^{-\frac{1}{2}} st_r^C (Re_r)^{\frac{1}{2}}$$

$$= \tfrac{1}{2} 2^{\frac{1}{2}} [(\phi/Pr_{eq})\tilde{h}_\eta]_{\eta=0}. \qquad (26)$$

The radiative Stanton number is defined as $st_r^R \equiv q_w^R/\frac{1}{2}\rho_r u_e^3$ where the radiative flux absorbed by the wall is $q_w^R = \int_0^{\infty} \varepsilon_\nu q_\nu^-(0) \mathrm{d}\nu$ and $q_\nu^-(0)$ is given by (18). In the optically thin limit

$$q_w^R = \varepsilon q^-(0) = \varepsilon 2\sigma \int_0^{\infty} \rho \kappa_P T^4 \mathrm{d}y, \qquad (27)$$

and

$$Q^R \equiv (2n+1)^{-\frac{1}{2}} \varepsilon^{-1} st_r^R (Re_r)^{\frac{1}{2}}$$

$$= 8^{\frac{1}{2}} s \int_0^{\infty} \tilde{\kappa}_P \tilde{T}^4 \mathrm{d}\eta. \qquad (28)$$

4.1 *Aspects of the hypersonic limit*

As discussed in Section 2, the enthalpy boundary conditions are approximated by $\tilde{h}_e = \tilde{h}_w = 0$ in the hypersonic limit. When the perfect gas law and the viscosity relationship $\tilde{\mu} = \tilde{T}^\omega (0 < \omega < 1)$ are used, or when more accurate analytic representations of the gas properties are used, it follows in the hypersonic limit (using the notation $(\ )_{e,w}$ for values at both the edge and the wall) that

$$\tilde{\rho}_{e,w} \to \infty, \quad \tilde{\mu}_{e,w} = 0, \quad \tilde{T}_{e,w} = 0, \quad \phi_{e,w} \to \infty, \qquad (29)$$

and thus

$$Re_{e,w} \to \infty, \quad (c_f)_{e,w} = 0, \quad st_{e,w}^C = 0.$$

From (21) and (22) it follows that $y(\eta = \infty) = \delta^*$, and from (23) and (24) that $\theta = 0$ and $\theta_H = 0$. The limiting behavior of the function $c_f Re^{\frac{1}{2}}$ may be derived from the relation

$$(c_f)_r Re_r^{\frac{1}{2}} = \phi_e^{\frac{1}{2}}(c_f)_e Re_e^{\frac{1}{2}} = \phi_w^{\frac{1}{2}}(c_f)_w Re_w^{\frac{1}{2}}. \qquad (30)$$

Since $(c_f)_r Re_r^{\frac{1}{2}}$ remains finite and non-zero as $M_e \to \infty$, it follows from (29) that $(c_f)_e Re^{\frac{1}{2}} \to 0$ and $(c_f)_w Re_w^{\frac{1}{2}} \to 0$ as $M_e \to \infty$. Similar results are obtained for $st^C Re^{\frac{1}{2}}$.

For large values of M_e it has been found (Sibulkin and Dispaux [13]) that u_η and h_η vary

rapidly near the wall, and it follows from (25), (26) and (29) that $u_\eta(0) \to 0$ and $h_\eta(0) \to 0$ as $M_e \to \infty$. (It may be noted that the corresponding limits in the physical plane are $u_y(0) \to \infty$ and $h_y(0) \to \infty$.) Thus it is no longer possible to obtain values for τ_w and q_w^C by numerical differentiation of the velocity and enthalpy profiles. To overcome this difficulty, formulas for obtaining skin friction and conductive heat transfer involving only integration of the velocity and enthalpy profiles have been developed.

5. INTEGRAL RELATIONS FOR F AND Q^C

The integral relation for F is derived by integrating each term of (13) from $\eta = 0$ to $\eta = \infty$. After integrating the second and fourth terms by parts and using (15) and (16) one obtains after some manipulation

$$-[\phi\tilde{u}_\eta]_{\eta=0} + \int_0^\infty \tilde{u}(1-\tilde{u})\mathrm{d}\eta + f(0,s) = -\frac{2s}{2n+1}\frac{\mathrm{d}}{\mathrm{d}s}\int_0^\infty \tilde{u}(1-\tilde{u})\mathrm{d}\eta - \frac{2s}{2n+1}f_s(0,s), \quad (31)$$

and using the definitions of Θ and F this becomes

$$F = \Theta + \frac{2s}{2n+1}\frac{\mathrm{d}\Theta}{\mathrm{d}s} + 2^{\frac{1}{2}}\left[f(0,s) + \frac{2s}{2n+1}f_s(0,s)\right]. \quad (32)$$

For an impermeable wall the term in brackets equals zero; when in addition the velocity profiles are similar, equation (32) reduces to $F = \Theta$ which is equivalent to the standard result $(c_f)_e = (2n+1)(\theta/x)$.

In deriving an integral relation for Q^C, simpler results may be obtained by working with the energy equation for the stagnation enthalpy H. After a derivation analogous to that leading to (14), the resulting equation* is

$$[(\phi/Pr_{eq})\tilde{H}_\eta]_\eta + f\tilde{H}_\eta + [\phi(1 - Pr_{eq}^{-1})(\tilde{u}^2)_\eta]_\eta = \frac{2s}{2n+1}(\tilde{u}\tilde{H}_s - f_s\tilde{H}_\eta) + \frac{2s}{\tilde{\rho}}\tilde{\nabla}\cdot\tilde{q}^R. \quad (33)$$

Termwise integration of (33) finally yields

$$-[(\phi/Pr_{eq})\tilde{h}_\eta]_{\eta=0} + \int_0^\infty \tilde{u}(\tilde{H}_e - \tilde{H})\mathrm{d}\eta + f(0,s)(\tilde{H}_e - \tilde{H}_w) = -\frac{2s}{2n+1} \times \frac{\mathrm{d}}{\mathrm{d}s}\int_0^\infty \tilde{u}(\tilde{H}_e - \tilde{H})\mathrm{d}\eta - \frac{2s}{2n+1}f_s(0,s) \times [\tilde{H}_e - \tilde{H}_w] + \int_0^\infty \frac{2s}{\tilde{\rho}}\tilde{\nabla}\cdot\tilde{q}^R\mathrm{d}\eta \quad (34)$$

and using the definitions of Θ_H and Q^C this becomes

$$Q^C = \frac{\Theta_H}{2} + \frac{2s}{2n+1}\frac{\mathrm{d}\Theta_H}{\mathrm{d}s} - 2^{\frac{1}{2}}\int_0^\infty \frac{s}{\tilde{\rho}}\tilde{\nabla}\cdot\tilde{q}^R\mathrm{d}\eta + \frac{1}{2^{\frac{1}{2}}}\left[f(0,s) + \frac{2s}{2n+1}f_s(0,s)\right](1 + \tilde{h}_e - \tilde{h}_w). \quad (35)$$

In the optically thin case, the use of (20) and (28) enables the radiation term to be expressed by

$$2^{\frac{1}{2}}\int_0^\infty \frac{s}{\tilde{\rho}}\tilde{\nabla}\cdot\tilde{q}^R\mathrm{d}\eta = 2Q^R \quad (35a)$$

where Q^R is given by (28). Equations (32) and (35) will be used to obtain numerical values of the

* The forms of (33) and (14) differ only in the terms involving viscous dissipation. Equation (33) has been used in a number of investigations of similar boundary layers where particularly simple results may be obtained when the assumption $Pr_{eq} = 1$ is made. When solutions are to be obtained by the method of finite differences, (33) has the disadvantage that its dissipation term contains a second derivative of $\tilde{u}$.

skin friction and conductive heat transfer parameters F and Q^c.

6. METHOD OF SOLUTION

Numerical solutions of (13)–(15) were obtained by the methods of finite differences. Successful use of this method requires that the algorithm employed be stable and convergent. Stability can be assured, independent of step size, by the use of an implicit difference scheme; and the well know Crank–Nicholson six-point scheme was used for this work.

In order to improve the convergence of the solutions a modified method of quasi-linearization was employed. The use of this method to solve sets of ordinary differential equations with two-point boundary conditions is described in Radbill and McCue [14] and has been used by them and others in the calculation of similar boundary-layer flows. The application of the method to a single partial differential equation is discussed by Kalaba [15]. We have used a modification of Kalaba's technique for our coupled set of partial differential equations as outlined below.

After isolating the highest order derivative G on the left-hand side, (13) and (14) can be written symbolically in the form

$$G = F(x_i), \quad i = 1, 2, \ldots, n \tag{36}$$

where in our case G is of the form $G = [\alpha z_\eta]_\eta$. An iterative scheme for solving (36) is obtained by writing it in the quasilinear form

$$G^{k+1} = F^k(x_i) + \sum_i \left[\frac{\partial F}{\partial x_i}\right]^k (x_i^{k+1} - x_i^k) \tag{37}$$

where k is the iteration number. The quasilinear contribution is given by the summation term; in its absence one has the usual Picard scheme of integration. Application of (37) to the momentum equation (13) gives

$$\begin{aligned}[\phi^k(\tilde{u}_\eta)^{k+1}]_\eta = &\left[\frac{2s}{2n+1}(\tilde{u}\tilde{u}_s - f_s\tilde{u}_\eta) - f\tilde{u}_\eta\right]^k \\ &+ \frac{2s}{2n+1}\tilde{\mu}_s^k(\tilde{u}^{k+1} - \tilde{u}^k) \\ &+ \frac{2s}{2n+1}\tilde{u}^k(\tilde{u}_s^{k+1} - \tilde{u}_s^k) \\ &+ \left[-\frac{2s}{2n+1}f_s - f\right]^k(\tilde{u}_\eta^{k+1} - \tilde{u}_\eta^k)\end{aligned} \tag{38}$$

when the x_i are chosen to be $\tilde{u}$, $\tilde{u}_s$ and $\tilde{u}_\eta$. It should be pointed out that f and f_s are not included in x_i because this would require knowledge of f after $(k+1)$ iterations in order to calculate the $(k+1)$ iterate of $\tilde{u}$; this is not possible since f is an integral of $\tilde{u}$. A corresponding treatment of the energy equation (14) using the optically thin form of the radiation term (20) gives

$$\begin{aligned}[(\phi/Pr_{eq})^k(h_\eta)^{k+1}]_\eta = &\left[\frac{2s}{2n+1}(\tilde{u}\tilde{h}_s - \tilde{f}_s\tilde{h}_\eta)\right. \\ &\left. - f\tilde{h}_\eta - 2\phi\tilde{u}_\eta^2 + 8s\tilde{\kappa}_P\tilde{T}^4\right]^k \\ &+ \left[32s\tilde{\kappa}_P\tilde{T}^3\frac{d\tilde{T}}{d\tilde{h}} + 8s\tilde{T}^4\frac{d\tilde{\kappa}_P}{d\tilde{h}}\right. \\ &\left. - 2\tilde{u}_\eta^2\frac{d\phi}{dh}\right](\tilde{h}^{k+1} - \tilde{h}^k) \\ &+ \frac{2s}{2n+1}\tilde{u}^k(\tilde{h}_s^{k+1} - \tilde{h}_s^k) \\ &+ \left[-\frac{2s}{2n+1}f_s - f\right]^k(\tilde{h}_\eta^{k+1} - \tilde{h}_\eta^k).\end{aligned} \tag{39}$$

Since $\tilde{T}$, $\tilde{\kappa}_P$ and ϕ are functions of $\tilde{h}$ they have been included in x_i; however neither $\tilde{u}$ nor its derivatives can be included in x_i when dealing with the energy equation.

Equations (38) and (39) are the quasilinear forms of the momentum and energy equations. They are reduced to their finite difference equivalents by application of the Crank–Nicolson scheme (e.g. Richtmyer and Morton [16]). The resulting tridiagonal matrices are solved by a Gaussian elimination algorithm given

by Douglas [17]. A detailed discussion of the method of solution is given in Dennar [18].

7. GAS PROPERTIES

In order to solve the conservation equations the thermodynamic, transport, and radiative properties of the gas must be specified. The properties used in the paper are those of air in local thermodynamic equilibrium. This assumption is expected to be well met when aerodynamic heating is important except in the region near the leading edge where non-equilibrium effects may be important.

Solutions have been obtained for two sets of gas properties which will be referred to as "exact gas" and "real gas" calculations. The "exact gas" calculations use the correlation equations of Viegas and Howe [19] for the properties of air in the temperature range 1000°C to 15000°C. The pressure levels used in this paper are 0·1, 1·0 and 10 atm; the property curves were extrapolated to lower temperatures when necessary.

As indicated in the Introduction, the use of exact gas properties requires a new solution of the boundary layer equations for each combination of u_e and p_e. Less accurate but more general solutions can be obtained by using power law approximations to the gas properties of the form

$$\tilde{\mu} = \tilde{h}^{\alpha}, \tilde{\rho} = \tilde{h}^{-\beta}, \tilde{T} = \tilde{h}^{\gamma}, \tilde{\kappa}_P = \tilde{h}^{\delta}; \qquad (40)$$

solutions obtained using (40) are referred to as "real gas" results. Once the values of $\alpha, \ldots, \delta$ and Pr_{eq} have been specified, the solution of the boundary layer equations in the hypersonic limit is independent of both u_e and p_e.

The exponents in (40) were chosen by plotting the correlation curves of Viegas and Howe [19] for the three values of p_e used on log–log coordinates and selecting the best straight line fit. The values chosen were

$$\alpha = 0{\cdot}4, \beta = 0{\cdot}8, \gamma = 0{\cdot}5, \delta = 3{\cdot}0. \qquad (41)$$

Since the curves of Pr_{eq} were neither independent of p_e nor linear, an average value of $Pr_{eq} = 0{\cdot}75$

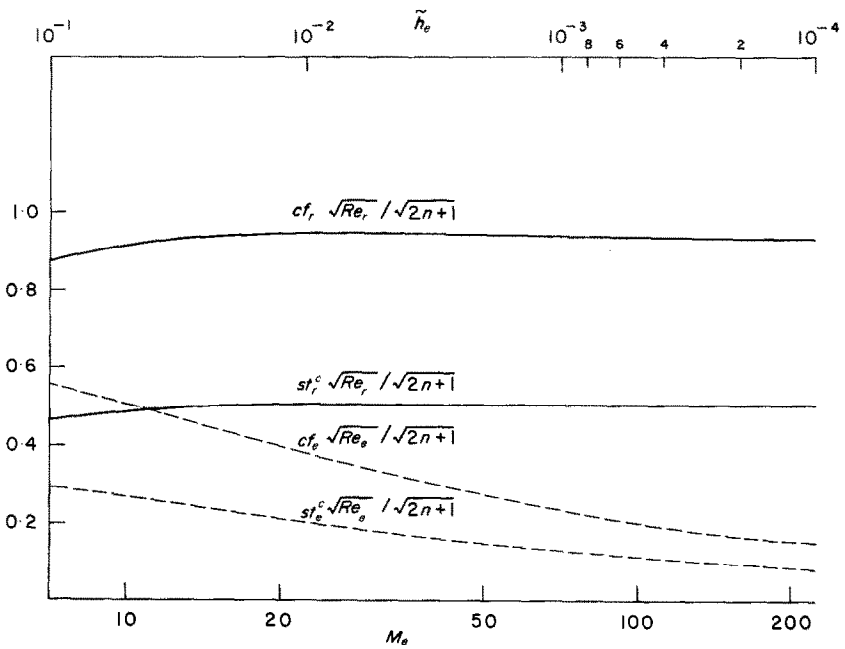

FIG. 1. Comparison of friction and heat transfer coefficients based on reference and edge values (non-radiating results, $\tilde{h}_w = \tilde{h}_e$).

was used. Figures showing these gas property curves are given in [18].

8. NUMERICAL RESULTS AND DISCUSSION

The boundary layer equations (13)–(15) with boundary conditions (16) and the optically thin approximation to the radiation term (20) were solved by the finite difference method discussed in section 6. Two groups of solutions will be discussed: (i) similarity solutions obtained by setting the radiation term in (14) equal to zero, and (ii) nonsimilar, radiating solutions. The nonradiating, similarity solutions serve two purposes. They provide skin friction and heat transfer results which are applicable at free-stream conditions for which radiation effects are unimportant, and they constitute the proper initial conditions for the radiating solutions. This result follows from the vanishing of the radiation term in (14) at $s = 0$.

The similarity solutions were generated using the finite difference method by marching downstream in s from an arbitrary initial profile until profiles invariant with s were obtained. (In practice, convergence was facilitated by starting with an approximately correct profile.) This procedure was judged to be more convenient than the usual practice of writing a separate

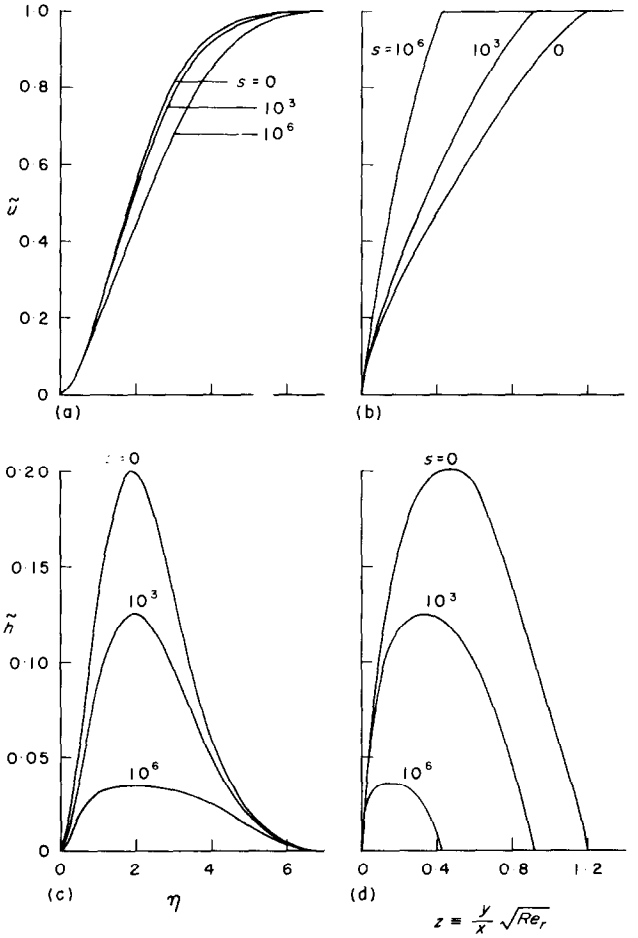

FIG. 2. Velocity and enthalpy profiles for radiating flow ($n = 0$).

program to solve the ordinary differential equations governing the similarity profiles.

Nonradiating, similarity solutions for skin friction and heat transfer using "real gas" properties are plotted in Fig. 1. The solutions are for the boundary condition $\tilde{h}_w = \tilde{h}_e$; the relationship between M_e and $\tilde{h}_e$ is $M_e^2 = [2/(\gamma - 1)]\tilde{h}_e^{-1}$. The results for c_f and st^C based on values at the edge of the boundary layer follow the established trend, i.e. they decrease monotonically with increasing M_e. The corresponding c_f and st^C results based on the reference values defined in section 2, however, approach constant values as $M_e \to \infty$ with an error of less than one per cent for $M_e > 20$. These results illustrate the existence of the hypersonic limit postulated in sections 1 and 4.1. The two sets of results are related by (30).

Numerical results for radiating boundary layers in the hypersonic limit $\tilde{h}_w = \tilde{h}_e = 0$ using

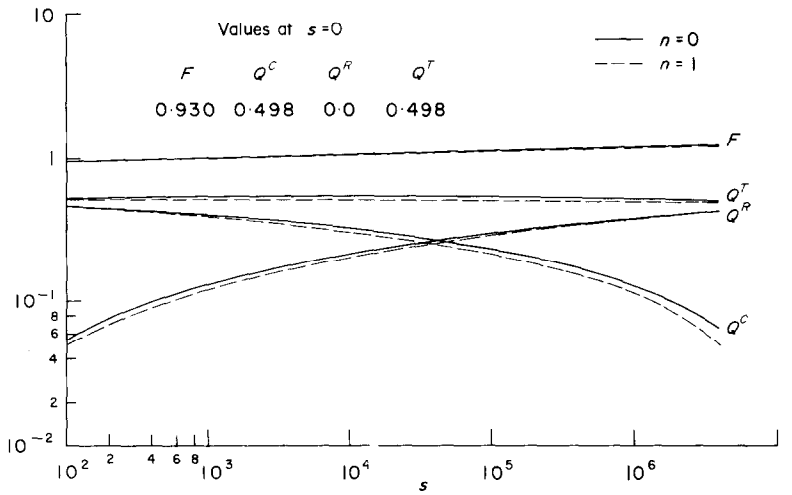

FIG. 3a. Friction and heat transfer parameters for radiating flow.

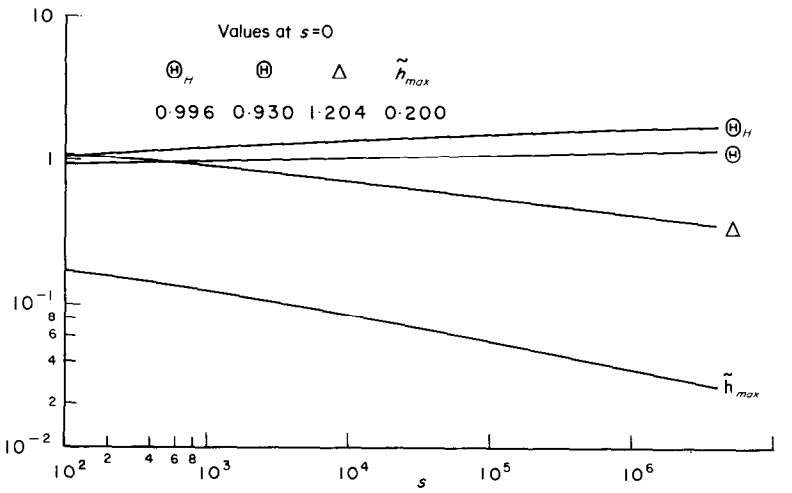

FIG. 3b. Boundary layer thicknesses and maximum enthalpy for radiating flow.

"real gas" properties will now be considered. The effect of radiation on the velocity and enthalpy profiles for planar flow are shown in Fig. 2. The results at $s = 0$ are those given by the similarity solutions as discussed above. The profiles are plotted against both the "transformed" coordinate η and the "physical coordinate z. As s increases, the boundary layer thickness decreases relative to that for nonradiating flow due to the loss of energy from the boundary layer by radiative transfer. This thinning of the compressible boundary layer due to radiation has been overlooked by some previous investigators who only considered profiles in the η-plane where the effect is absorbed in the transformation from y to η. The loss of energy due to radiative transfer also causes the maximum enthalpy in the boundary layer to continually decrease as s increases. This causes a flattening of the enthalpy profile although the effect is not as pronounced as previously found for perfect gas properties (Sibulkin and Dispaux [13]) In addition it is observed that the edge of the boundary layer in the physical plane is quite sharp.

Further results for the radiating "real gas" boundary layer are shown on Fig. 3. As noted in section 2, the transformed equations for planar ($n = 0$) and axisymmetric ($n = 1$) radiating flows are not identical. The resulting numerical differences as shown by the curves of Fig. 3a are small; for the parameters plotted on Fig. 3b there is no discernable difference between the curves for $n = 0$ and $n = 1$. It should be borne in mind however that for axisymmetric flow a $\sqrt{3}$ factor has been absorbed in the parameter definitions. For the convenience of the reader, the values at $s = 0$ have been listed on the figures.

From Fig. 3a it can be seen that radiation has only a minor effect on the friction parameter F. The conductive heat transfer Q^C decreases with increasing s due to radiative cooling while the radiative contribution Q^R increases as the boundary layer thickens. A surprising result, however, is that the parameter $Q^T(\equiv Q^C + Q^R)$ remains nearly constant for all values of s showing that the total heat flux reaching the wall at a given location is almost independent of the various physical processes going on in the boundary layer. (However, the heat absorbed by the wall depends on its emissivity ε.) The momentum and energy integral parameters Θ and Θ_H shown on Fig. 3b increase slowly with s while the displacement thickness parameter Δ decreases due to the increase in density resulting from radiative cooling. The maximum enthalpy in the boundary layer decreases with increasing s as mentioned in the discussion of Fig. 2.

It may be worthwhile to emphasize that the results shown on Figs. 2 and 3 are "universal curves" for the hypersonic boundary layer in the sense of being independent of external flow conditions. The primary limitation on their accuracy is the use of the approximate "real gas" properties. The errors due to this approximation will now be discussed by comparing these results with solutions of the boundary layer equations using exact gas properties. Such a comparison for friction and heat transfer values at $s = 0$ (nonradiating, similarity solutions) is shown on Fig. 4. The agreement between our "real gas" and exact gas values is within 6 per cent. Also included on the plot are results obtained by Chapman [20] using the same exact gas properties for $h_e = 0{\cdot}075$ and several wall conditions. The agreement with the "real gas" results is good except for the calculations performed at $p_e = 0{\cdot}1$ atm for the higher velocities. Here Chapman's results are up to 11 per cent lower for F and 15 per cent lower for Q^C than the "real gas" values. A check on Chapman's calculations for this particular pressure using the same boundary conditions as he did was performed and our results for F and Q^C were within 6 per cent and 2 per cent respectively of the "real gas" values. The discrepancy between the two calculations is attributed to the different methods used to integrate the boundary layer equations.

Representative nonradiating profiles for "exact" and "real" gases are shown in Fig. 5

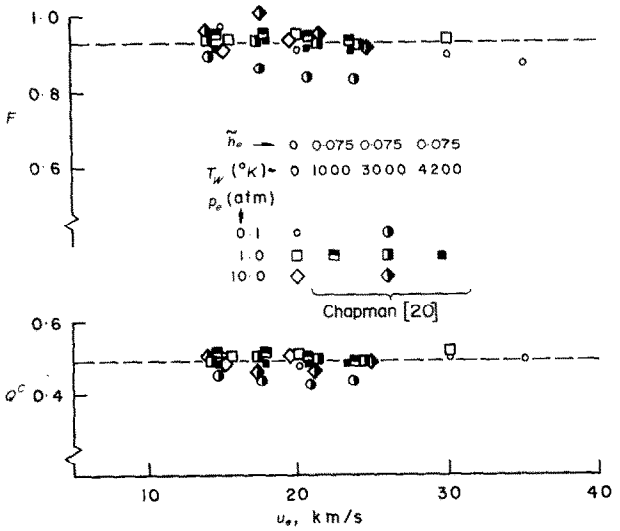

FIG. 4. Comparison of friction and heat conduction parameters for "real" and "exact" gases (non-radiating results).

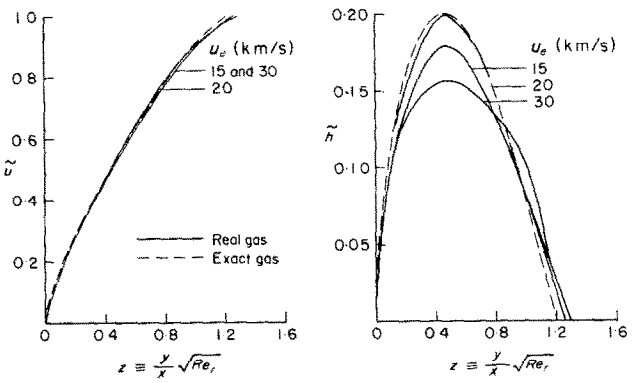

FIG. 5. Comparison of velocity and enthalpy profiles for "real" and "exact" gases (non-radiating results, $p_e = 1$ atm).

for $p_e = 1$ atm. The velocity profiles for the two cases are almost indistinguishable whereas the difference in the enthalpy profiles is apparent. The agreement of the velocity profiles is a clear indication of the weak coupling between the momentum and energy equations. In spite of the differences in enthalpy values, the integrated heat flux parameter Q^C is almost constant (cf. Fig. 4) and hence appears to be insensitive to the details of the enthalpy profiles.

A comparison between the "real" and "exact" gas friction and heat transfer parameters for $s > 0$ at $p_e = 1$ atm is shown in Fig. 6. These calculations show that the effects of radiation may be neglected for $s < 10$. The significance of this result for practical applications will be discussed later. For $s > 10$, the exact gas results depend upon u_e and the accuracy of the "real gas" results decreases as u_e decreases. These errors are primarily due to the "real gas"

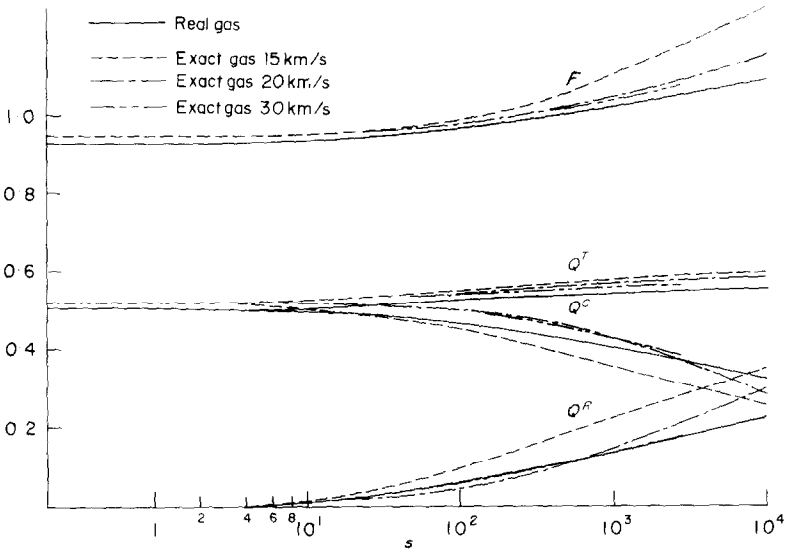

FIG. 6. Comparison of friction and heat transfer parameters for "real" and "exact" gases ($p_e = 1$ atm).

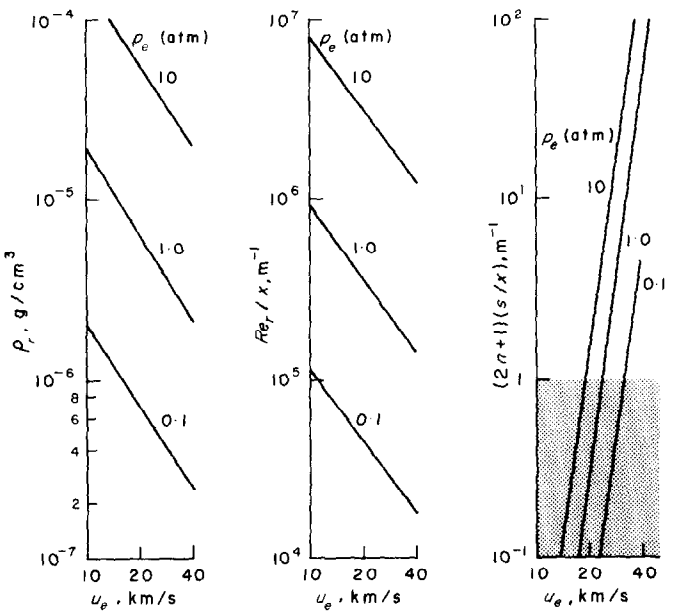

FIG. 7. Values of reference quantities. (For $x < 10$ m, boundary layer radiation effects may be neglected for values of $(2n + 1)(s/x)$ in the shaded region).

approximation for κ_P which was chosen to match the exact gas values at high enthalpy levels but which substantially underestimates the exact values at low values of h. Since the enthalpy levels in the boundary layer decrease with decreasing u_e, the resulting errors in the friction and heat transfer parameters increase as u_e decreases.

In order to apply the results given in this paper to the calculation of values of τ, q^C and q^R for design purposes, values of the reference quantities ρ_r, Re_r and $(2n+1)(s/x) \equiv \Gamma_r \rho_r (\kappa_P)_r$ must be used. Values of these quantities calculated from (40), (41), and the "standard states" given in Table II of Viegas and Howe [19] are plotted in Fig. 7.*

In connection with Fig. 6 it was found that the effects of radiation can be neglected for $s < 10$. For wedges and cones less than 10 m long it follows that radiation may be neglected when $(2n+1)(s/x) < 1$ m^{-1} as indicated in Fig. 7. However calculations of Earth reentry trajectories including returns from the far solar system (Howe and Schaeffer [21]) show that u_∞ and p_∞ will not exceed values of 15 km/s and 10^{-2} atm, and that for all wedge or cone angles the resulting values of u_e and p_e give $(2n+1)(s/x) < 1$ m^{-1}. Thus it may be concluded that radiation effects on boundary layer friction and heat transfer to wedges and cones may be neglected for flight in the Earth's atmosphere.† It should not be forgotten, however, that when the wedge or cone angle is large there will be significant radiative transfer to the body from the hot, inviscid shock layer (Olstad [22]).

In the light of the above conclusion, the results for nonradiating flow take on added significance. Consequently, additional solutions of the nonradiating boundary layer equations were obtained for a range of values* of $\tilde{h}_e$ and $\tilde{h}_w$ to determine the range of validity of the values of F and Q^C obtained in the hypersonic limit $\tilde{h}_e = 0, \tilde{h}_w = 0$. These results are given in Table 1 (which includes values for $\tilde{h}_e = \tilde{h}_w$ shown on Fig. 1). The "real gas" calculations given in Table 1 and the comparison of "real gas" and "exact gas" results shown in Fig. 4 may be combined to conclude that for air in the range $\tilde{h}_e < 0{\cdot}1$, $\tilde{h}_w < 0{\cdot}1$, $u_e < 15$ km/s, $0{\cdot}1 < p_e < 10$ atm, the hypersonic limiting values of $F = 0{\cdot}93$ and $Q^C = 0{\cdot}50$ can be used with an error of less than 15 per cent. It is hoped that this fairly general result will be sufficiently accurate for many design studies.

Table 1. Value of the convective heat transfer parameter Q^C for several combinations of $\tilde{h}_e$ and $\tilde{h}_w$

$\tilde{h}_w$	$\tilde{h}_e$ 0	0·05	0·10
0	0·50	0·52	0·53
0·05	0·46	0·48	0·49
0·10	0·42	0·44	0·46

ACKNOWLEDGEMENT

This work was partially supported by the National Science Foundation through NSF Grant GK-16535 and NSF Grant GJ-409.

REFERENCES

1. H. BLASIUS, Grenzschichten in Flüssigkeiten mit kleiner Reibung, *Z. Math. Phys.* **56**, 1–37 (1908). (Translated in NACA TM 1256.)
2. K. POHLHAUSEN, Zur näherungsweisen Integration der Differentialgleichung der laminaren Grenzschicht, *Z. Angew Math. Mech.* **1**, 252–268 (1921).

* Reference values are also used in the "exact gas" calculations to obtain $\tilde{\rho}$ and the other nondimensional gas properties, where, for example,

$$\tilde{\rho} = \frac{(\rho)_s}{\rho_r} \frac{\rho}{(\rho)_s}$$

and the $(\,)_s$ values are the "standard states" of Viegas and Howe.

† Although the present numerical solutions do not include atomic lines in the radiative transfer term, the addition of these lines would be equivalent at most to doubling κ_P. This would not alter the conclusion stated above.

* When the hypersonic approximations $h_\infty = 0$ and $u_e = u_\infty \cos\theta$ are used, the value of $\tilde{h}_e$ is given by $\tilde{h}_e = \tan^2\theta$ where θ is the wedge or cone semi-vertex angle. The value of h_w must be calculated from T_w, p_e, u_∞ and θ.

3. E. R. VAN DRIEST, Investigation of laminar boundary layer in compressible fluids using the Crocco method, NACA TN 2597, (1952).
4. TH. VON KÁRMÁN and H. S. TSIEN, Boundary layer in compressible fluids, *J. Aero. Sci.* **5**, 227–233 (1938).
5. K. STEWARTSON, *The Theory of Laminary Boundary Layers in Compressible Fluids*. Oxford University Press, Oxford (1954).
6. D. R. CHAPMAN and M. W. RUBESIN, Temperature and velocity profiles in the compressible laminar boundary layer with arbitrary distribution of surface temperature, *J. Aero. Sci.* **16**, 547–565 (1949).
7. W. H. DORRANCE, *Viscous Hypersonic Flow*. McGraw-Hill, New York (1962).
8. N. B. COHEN, Boundary layer similar solutions and correlation equations for laminar heat transfer distribution in equilibrium air at velocities up to 41,000 feet per second, NASA TR R-118 (1961).
9. C. B. COHEN and E. RESHOTKO, Similar solutions for the compressible laminary boundary layer with heat transfer and pressure gradient, NACA TN 3325 (1956).
10. L. LEES, Laminar heat transfer over blunt-nosed bodies at hypersonic flight speeds, *Jet Propulsion* **26**, 259–269 (1956).
11. J. T. HOWE and J. R. VIEGAS, Solutions of the ionized radiating shock layer, including reabsorption and foreign species effects, and stagnation region heat transfer, NASA TR R-159 (1963).
12. E. M. SPARROW and R. D. CESS, *Radiation Heat Transfer*. Brooks/Cole, Belmont, California (1966).
13. M. SIBULKIN and J.-C. DISPAUX, Numerical solutions for radiating hypervelocity boundary-layer flow on a flat plate, *AIAA Jl* **6**, 1098–1104 (1968).
14. J. R. RADBILL and G. A. MCCUE, *Quasilinearization and Nonlinear Problems in Fluid and Orbital Mechanics*. American Elsevier, New York (1970).
15. R. KALABA, On nonlinear differential equations, the maximum operation, and monotone convergence. *J. Math. Mech.* **8**, 519–574 (1959).
16. R. D. RICHTMYER and K. W. MORTON, *Difference Methods for Initial Value Problems*. Interscience, New York (1967).
17. J. DOUGLAS, JR., The numerical solution of elliptic and parabolic differential equations, *Survey of Numerical Analysis*. McGraw-Hill, New York (1962).
18. E. A. DENNAR, Radiating hypervelocity boundary layers, Ph.D. Thesis, Brown University, Providence, R. I. (1970).
19. J. R. VIEGAS and J. T. HOWE, Thermodynamic and transport property correlation formulas for equilibrium air from 1,000°K, NASA TN D-1429 (1962).
20. G. T. CHAPMAN, Theoretical laminar convective heat transfer and boundary-layer characteristics on cones at speeds up to 24 km/s, NASA TN D-2463 (1964).
21. J. T. HOWE and Y. S. SHEAFFER, Effects of uncertainties in the thermal conductivity of air on convective heat transfer for stagnation temperature up to 30,000°K, NASA TN D-2678 (1965).
22. W. B. OLSTAD, Nongray rediating flow about smooth symmetric bodies, *AIAA Jl* **9**, 122–130 (1971).

COUCHES LIMITES RAYONNANTES À DES VITESSES D'ENTRÉE PLANÉTAIRES

Résumé—On présente des résultats pour couches limites laminaires à pression constante et à des vitesses où le rayonnement thermique peut être important. Quand les effets de rayonnement sont significatifs, les profils de la couche limite sont non-similaires et différentes solutions peuvent être obtenues pour des écoulements plans (plaques planes, coin) et des écoulements axisymétriques (cônes). En utilisant des approximations en loi puissance pour les propriétés du gaz et un nouvel ensemble de conditions de référence, on définit une limite hypersonique qui donne le frottement superficiel et les paramètres de transfert thermique indépendants du nombre de Mach. Pour un gaz particulier et une géométrie d'écoulement (plane ou axisymétrique), cette approche donne une solution universelle pour la couche limite rayonnante. On a trouvé que, bien que les flux thermiques convectifs et rayonnants varient fortement avec la distance au bord d'attaque, le flux thermique total est presque indépendant de la position. Pour des trajectoires d'entrée terrestre tenant compte des retours à partir du système solaire éloigné, on montre que la convection est le mode dominant du transfert thermique dans de telles couches limites pour des véhicules de taille modérée. On présente des comparaisons de la solution à partir des propriétés en loi puissance avec des calculs utilisant les propriétés exactes des gaz pour l'air et on discute le domaine d'accord.

STRAHLENDE GRENZSCHICHTEN BEI PLANETAREN EINTRITTSGESCHWINDIGKEITEN

Zusammenfassung—Es werden Ergebnisse angegeben für laminare Grenzschichten unter konstantem Druck für Geschwindigkeiten, bei denen thermische Strahlung wichtig sein kann. Falls Strahlungseffekte eine Rolle spielen, sind die Grenzschichtprofile nicht ähnlich, und man muss unterschiedliche Lösungen erhalten für ebene (ebene Platte, Keil) und achsensymmetrische (Kegel) Strömungen. Indem man die Gasstoffwerte durch einen Potenzansatz annähert und einen neuen Satz von Referenzzuständen benützt, wird ein Überschallgrenzfall definiert, der Parameter für die Oberflächenreibung und den Wärmeübergang

liefert, die unabhängig von der Mach-Zahl sind. Für ein spezielles Gas und eine Strömungsgeometrie (eben oder aschsensymmetrisch) liefert dieser Ansatz eine universelle Lösung für die strahlende Grenzschicht. Es ergibt sich, dass der totale Wärmestrom fast unabhängig von der Lage ist, obwohl der konvektive und der radiative Anteil sich mit der Entfernung von der Vorderkante stark ändern. Es wird gezeigt, dass für irdische Wiedereintrittsbahnen, einschliesslich der Rückkehr vom fernen Sonnensystem, die Konvektion die dominierende Form des Wärmeüberganges in derartigen Grenzschichten bei Fahrzeugen von mässiger Grösse ist. Es werden die Lösungen bei Stoffwerten mit Potenzansatz verglichen mit Rechnungen, die die exakten Stoffwerte von Luft benutzen, und der Bereich der Übereinstimmung wird diskutiert.

ИЗЛУЧАЮЩИЕ ПОГРАНИЧНЫЕ СЛОИ ПРИ СКОРОСТЯХ ВХОДА В АТМОСФЕРУ ПЛАНЕТ

Аннотация—Представлены результаты анализа ламинарных пограничных слоёв при постоянном давлении и скоростях, когда излучение становится заметным. Если эффекты излучения существенны, профили пограничного слоя неподобны, и решения для плоского (плоские пластины, клины) и осесимметричного (конусы) течений различны. Путём применения аппроксимации по степенному закону к свойствам газов, а также новых краевых условий, определяется сверхзвуковой предел, дающий независимые от числа Маха параметры поверхностного трения и теплообмена. Для определённого газа и геометрии течения (плоской или осесимметричной) этот подход даёт универсальное решение для излучающего пограничного слоя. Найдено, что хотя конвективный и лучистый тепловые потоки сильно изменяются с расстоянием от передней кромки, общий тепловой поток не зависит от положения. Показано, что для траекторий входа в атмосферу Земли, включая возвращения из далекой солнечной системы, конвекция является доминирующим видом теплообмена в таких пограничных слоях для кораблей среднего размера. Приводится сравнение решения для свойств, изменяющихся по степенному закону, с расчетами, использующими точные свойства газа, для воздуха и обсуждается степень их соответствия.